Angular-dependent metal-enhanced fluorescence from silver island films

Kadir Aslan, Stuart N. Malyn, Chris D. Geddes *

*Institute of Fluorescence, Laboratory for Advanced Medical Plasmonics and Laboratory for Advanced Fluorescence Spectroscopy,
Medical Biotechnology Center, University of Maryland Biotechnology Institute, 725 West Lombard Street, Baltimore, MD 21201, United States*

Abstract

In this Letter we report the observation of angular-dependent metal-enhanced fluorescence (MEF) from fluorophores deposited onto silver island films (SiFs). When illuminated with laser light (473 nm) at angles of 45° and 90° from the surface, SiFs scattered light at wide observation angles biased by the direction of the incident light. We observed angular-dependent MEF (10-fold) from FITC-HSA immobilized onto the SiFs, again slightly biased with respect to the direction of the incident light. We also measured the photostability of FITC from the back of the glass substrate at angles of 225° and 340°.
© 2008 Elsevier B.V. All rights reserved.

1. Introduction

Since the first experimental demonstration by Drexhage [1,2] that the spontaneous emission rate of fluorescent species could be modified by changing the local photonic mode density (PMD) by metal surfaces, there has been numerous studies to describe the interactions of fluorophores with metals placed in close proximity [3,4]. One can find a detailed summary of fluorescence near interfaces in a review article by Barnes [5]. When placed near a planar metal surface, the spontaneous emission of a single emitter (atom or molecule) follows a radiative and/or a non-radiative decay channel and is mainly dependent on the distance (R) between the emitter and the metal as well as the orientation of the dipole of the emitter with respect to the metal surface [6]. Two effects can be expected as a result of the distance dependence of the emission rate: (i) the emission rate oscillates as the distance is increased as the phase of the reflected field changes with distance and (ii) the strength of the oscillation decreases since the dipole emitter is a

point source. The relevance of dipole orientation can be seen when we consider the reflecting (metal) surface produces an image dipole on the metal surface. For a very small distance between the emitter and the metal surface, a dipole that is parallel to the surface is cancelled out by its image and a perpendicular dipole is enhanced. In this regard, the distance dependent spontaneous emission rate can be predicted assuming that the reflecting surface is perfect and the dipole moment of the emitter rotates rapidly within the emission lifetime.

It is important to note that the processes summarized above were derived for planar metal geometries, and one can find studies in the literature offering a description and applications of spontaneous emission rate near metallic nanoparticles similar to the description for planar metal geometries [7–15]. The major difference between the planar systems and particulate systems is the inclusion of localized modes occurring in particles. The localized modes in particulate systems results in the omission of the oscillations of decay rate observed for the planar systems. The frequency of the localized modes depends on the both the size and the shape of the metallic nanoparticles. For a single emitter placed near metal nanoparticles (using a dipole–dipole model) the non-radiative decay rate is shown to follow

---

* Corresponding author. Fax: +1 410 706 4600.
E-mail address: geddes@umbi.umd.edu (C.D. Geddes).

an R^{-6} dependence, the radiative decay rate follows an R^{-3} dependence and is also dominated by a dipole polarizability of the metallic nanoparticle [10]. It was also reported that the energy partially transferred (non-radiative coupling) from the excited state of the fluorescent species to surface plasmons of the metallic nanoparticles is then radiated by the nanoparticles themselves [16]. The extent of the radiation of the coupled energy by the metallic nanoparticles is also thought to be related to the scattering efficiency of metallic nanoparticles [17,18].

In recent years there has been resurgence in the number of papers published on metal–fluorophore interactions, given the ever-growing understanding of these interactions. One particular application is called metal-enhanced fluorescence (MEF) [19], where the fluorescence emission of fluorescent species is significantly increased by metal nanoparticles [20,21]. In almost all of these reports of MEF, different shapes and deposition techniques are used to deposit plasmonic nanoparticles on a surface and the fluorescence emission (quantum yield), lifetime and photostability are measured using front-face geometry (excitation and emission in the same front space as the plasmonic nanoparticles, i.e., on the same side as any support used). However, a recent report by Kawasaki et al. [22] shows that fluorescence emission from a fluorophore placed in close proximity to thick silver island films (prepared by sputtering) also couples into the mica substrate and is emitted in an angular-dependent fashion from back of the film. Our research group also reported similar observations from gold nanoparticle-deposited glass surfaces [23], which originated from our previous observations on angular-dependent scattering from gold colloids [24]. We reasoned that since the plasmonic nanoparticles are efficient in scattering light in an angular-dependent fashion (as predicted from Mie and Maxwell theories) and that the MEF phenomenon is directly related to the plasmon scattering of coupled-light, MEF would also be angular-dependent.

In this communication, we continue to build on our angular-dependent MEF studies and report our initial observations on angular-dependent light scattering and MEF from SiFs (deposited chemically onto a glass substrate). In this regard, we show that when illuminated at excitation angles of 45° and 90° (front-face geometry, separate experiments), SiFs scatter light an order-of-magnitude larger than glass substrates without SiFs, in an angular-dependent fashion, the scattering distribution observed to be slightly biased by the direction of the excitation light. We observed angular-dependent emission from FITC-HSA when coated onto SiFs and when excited at 45° and 90°, the fluorescence intensity spatial distribution are very similar to the plasmon light scattering by the nanoparticles themselves, i.e., with no fluorophore. We have also measured the photostability of FITC at different observation angles and show that FITC has similar photostabilities at these angles.

2. Experimental

Silver island films (SiFs) were prepared according to our previously published procedure [25]. The angular-dependent light scattering from glass and SiFs and the angular-dependent fluorescence spectra of FITC-HSA on glass and SiFs were collected using a setup described in one of our previous publications [23]. In short, a rotating stage (Edmund Scientific) is modified to hold a glass microscope slide and fiber optic mount. A laser line (at 473 nm) was used to illuminate the glass and SiFs for scattering studies and FITC-HSA for MEF studies at two excitation angles, i.e., 45° and 90° excitation. The angular-dependent scattering and the angular-dependent emission (through an emission filter, 488 nm razor edge) was then collected between the angles of 0–360°, except those angles obstructed by the fiber holder, Fig. 1.

The real-color photographs of FITC-HSA on SiFs and glass slides were taken with a Canon digital camera (3.2 Mega Pixel, 10× optical zoom) using the same razor-edge filter that was used for the emission spectra.

3. Results and discussion

It was previously reported that for the MEF phenomenon, the observed enhanced emission from a fluorophore-plasmonic nanoparticle 'system' is directly related to the efficiency of the non-radiative energy transfer from the fluorophores to the plasmonic nanoparticles, and the subsequently scattering efficiency of the plasmonic nanoparticles [16]. The evaluation of any substrate coated with plasmonic nanoparticles for MEF is usually undertaken by measuring the fluorescence emission intensity and lifetimes from these substrates, with and without the nanoparticles. Since these measurements are performed on the same side (same space) as the plasmonic nanoparticles and the fluorophores, the extent of MEF, for the most part, does not depend on the refractive index of the substrate. On the other hand, when the detector is positioned at the back of the substrate, the refractive index of the substrate becomes important: since the emission intensity now depends on the degree of coupling of fluorescence emission from the 'system' into the substrate where the
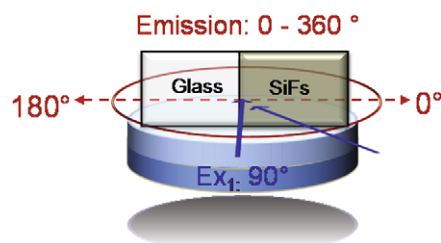

Fig. 1. Experimental setup for collecting angular-dependent emission/scattering from glass and silvered glass, as well as FITC-HSA coated glass and silvered glass. Only one excitation angle was used for each separate experiment. Ex: excitation. Emission was collected at 0–360°.

nanoparticles are deposited. In this regard, for angular-dependent MEF measurements, it is important to predict and/or experimentally determine the interaction of light (excitation and emission) with the plasmonic nanoparticle-deposited substrates.

Fig. 2 shows the polar plots for the scattering of p-polarized light (473 nm laser) from uncoated glass (control substrate without plasmonic nanoparticles) and SiFs deposited glass substrates, where the light propagated at two different angles, 45° and 90° on the same side as the SiFs. We note that the angles for the excitation light employed here are common in fluorescence spectroscopy for planar surfaces. The illumination with p-polarized light on glass and SiFs results in mostly p-polarized scattering of light that is slightly biased with respect to the angle of the incident light. The intensity of scattered light from the SiFs is approximately 10 times larger, and observed at much wider angles than that from glass at both illumination angles. This is due to the fact that silver nanoparticles are very efficient in scattering light in an angular-dependent fashion

[26]. Since the crux of this study is to utilize the scattering efficiency of silver nanoparticles after the interaction of illumination light or coupled fluorescence with the nanoparticles, we did not attempt to position the excitation source on the back of the substrate.

Fig. 3 shows the polar plots for fluorescence emission of FITC-HSA from glass and SiFs when excited at 45° and 90° (separate experiments) on the same side as the SiFs and FITC-HSA. We note that the emission intensities at 30–70° and 50–100° were not collected due to the experimental constraints when the excitation angle was at 45° and 90°, respectively. The angular-dependent fluorescence emission from SiFs was larger than the emission from glass for both excitation angles and appears biased with respect to the angle of incident light. This can be seen by comparing the intensity distribution in Fig. 3-top-left and bottom-left. At first this reproducible result was surprising, as isotropic fluorescence emission or emission following the Lambert's cosine law [27] for the substrates would be expected. The real-color photographs show the fluorescence
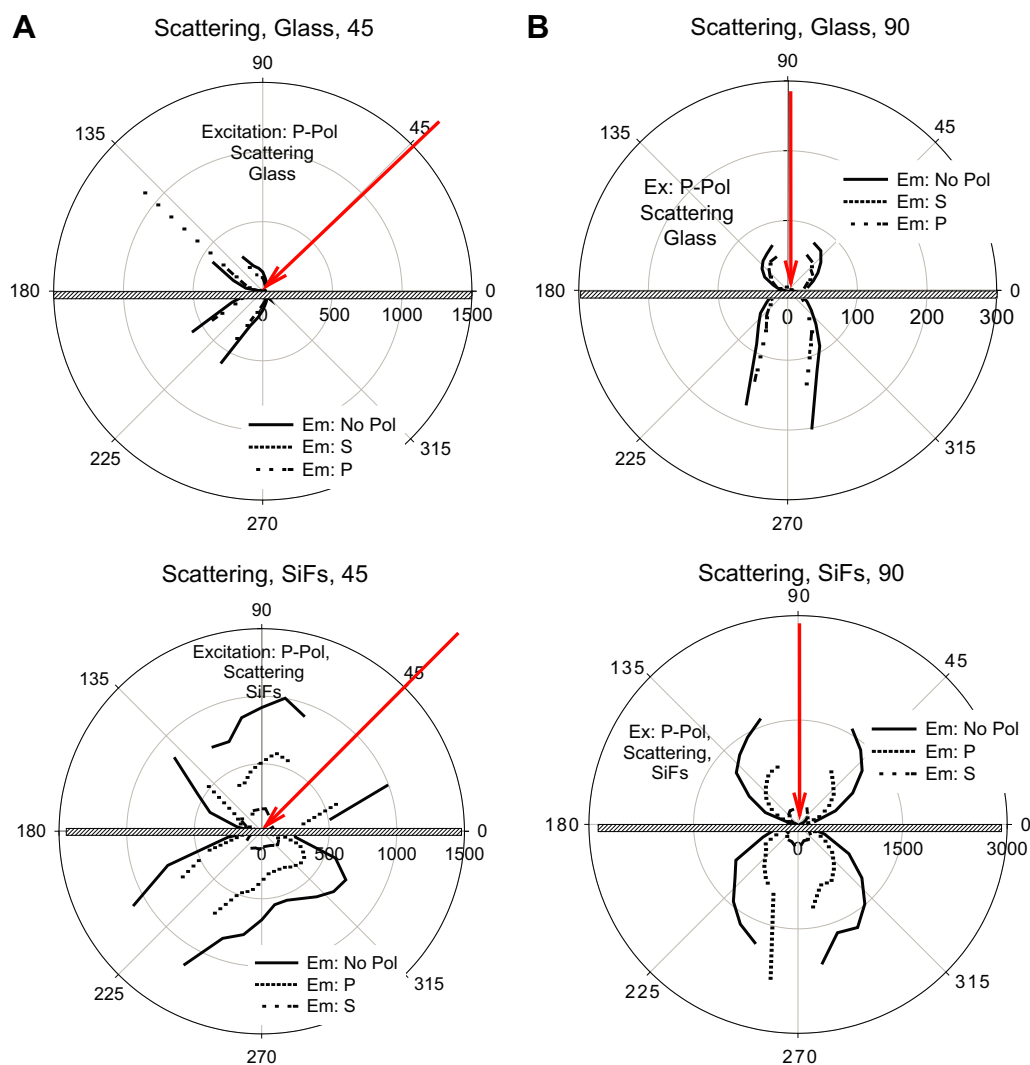

Fig. 2. Polar plots for the scattering of 473 nm laser light from glass and SiFs at (A) 45° and (B) at 90°.
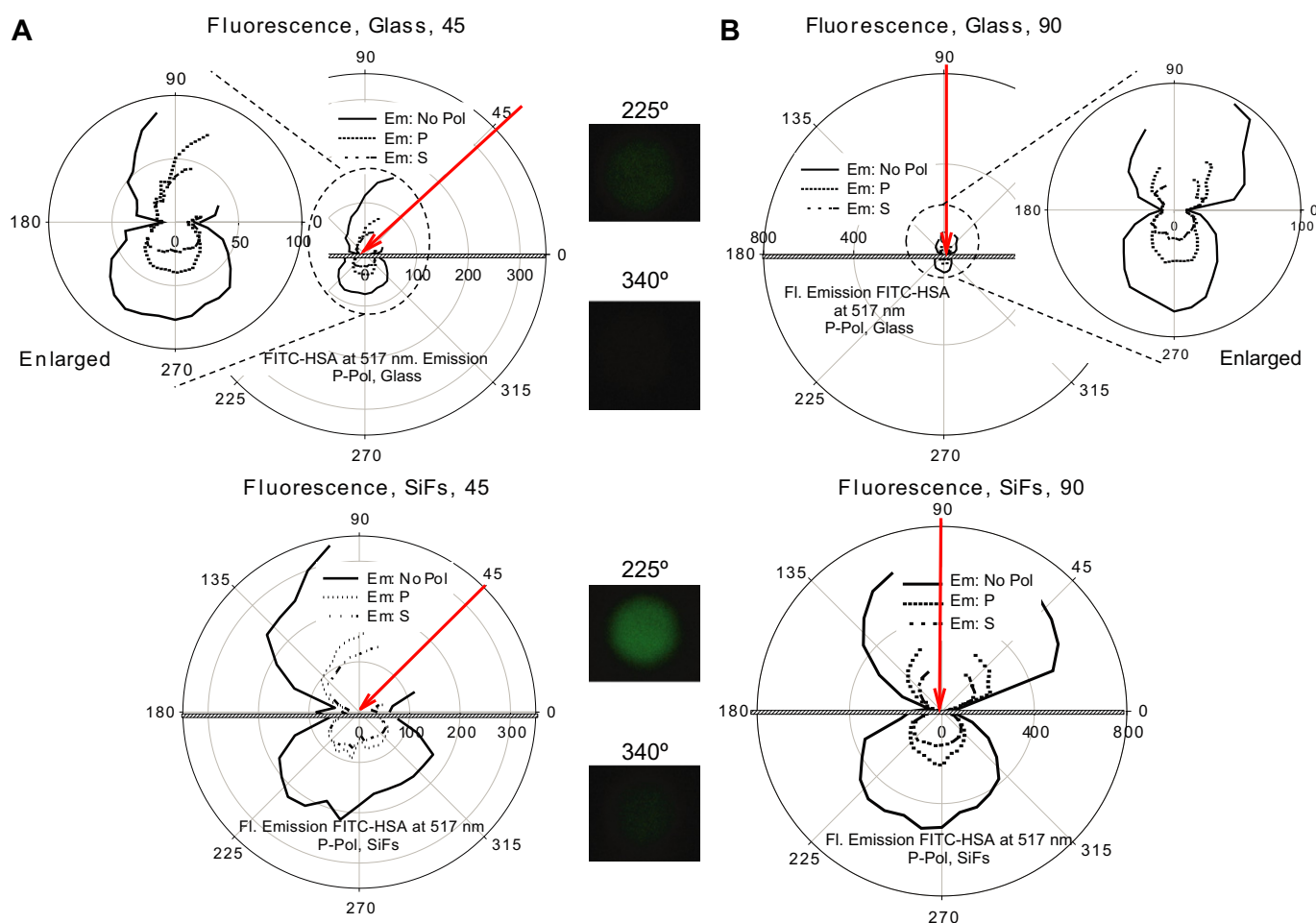
Fig. 3. Polar plots for fluorescence emission of FITC-HSA from glass and SiFs at (A) 45° and (B) at 90° taken through a razor edge filter. Real-color photographs show the fluorescence emission from FITC-HSA taken through a 488 nm emission filter at 225° and 340°. (For interpretation of the references in colour in this figure legend, the reader is referred to the web version of this article.)

emission from FITC-HSA from SiFs is brighter than that from glass as taken through a 488 nm emission filter at the two angles, 225° and 340°, on the back of the substrate.

Fig. 4A shows a polar plot for the calculated angular fluorescence enhancement factor, the emission intensity of FITC-HSA at 517 nm from SiFs divided by the emission intensity from glass, for both excitation angles. MEF factors vary between 3–5 and 3–10 for the excitation angle of 45° and 90°, respectively. We note that this polar plot is not likely to be the true enhancement factor plot, as the spatial distributions of fluorescence (glass) and coupled fluorescence (SiFs) are different. That said the plot does represent the absolute intensity increase as a function of angle. Typical fluorescence spectra of FITC-HSA on SiFs, Fig. 4A-bottom are observed from both the front and the back of the glass substrate, which indicates that the spectral shape of free-space and plasmon-coupled emission are virtually identical.

It was previously reported that the angular-dependent scattering of light from surfaces can be explained by Lambert's cosine law, based on the assumption that glass is a Lambertian surface [27]. According to the Lambert cosine

law, the intensity of scattered light, $I(\varphi)$, at an angle φ from the normal to the surface is represented by [27]

$$I(\phi) = I_0 \cos \phi \quad (0 \leq \phi \leq \pi/2) \tag{1}$$

Then, the angular-dependent scattered intensity from the back of the glass is governed by [27],

$$I_2(\phi) = \left(\frac{1}{n_2^2}\right) I_0 |\cos \phi| \quad (\pi/2 \leq \phi \leq \pi) \tag{2}$$

where n_2 is the refractive index of glass. According to Eq. (2), the light initially scattered into the glass also follows the cosine law but was 2.28 (square of $n_2 = 1.51$) times larger than the intensity detected in the backspace.

The scattering of light by subwavelength metallic nanoparticles themselves is angular-dependent. [28] For incident polarized light, the intensity of angular-dependent light scattered, $I_{scatt,}$ in the direction φ (angle) by a homogeneous spherical particle with radius $a \ll \lambda$ (wavelength of light), of the incident beam, is also polarized and is described by the Rayleigh expression [26,28];

$$I_{scatt} = \frac{16\pi^4 a^6 n_{med}^4 I_0}{r^2 \lambda^4} \left| \frac{m^2 - 1}{m^2 + 1} \right| \cos^2 \phi \tag{3}$$
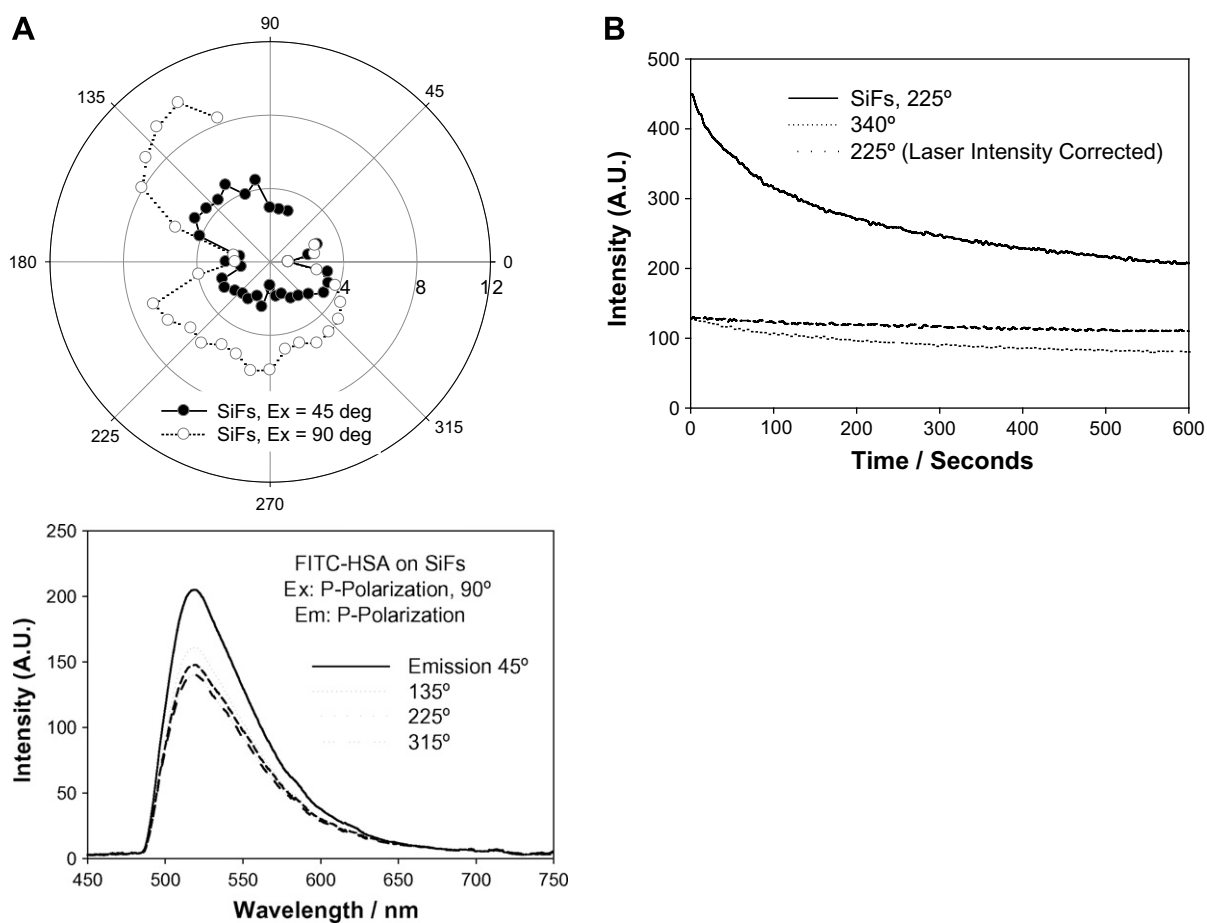
Fig. 4. Polar plot for (A) fluorescence enhancement factor, i.e., the ratio of emission intensity of FITC-HSA at 517 nm on silver films and the emission intensity of FITC-HSA on glass slides, typical angular-dependent fluorescence spectrum of FITC-HSA on SiFs (bottom), (B) photostability of FITC-HSA from SiFs. Emission intensity (p-polarized) was measured at 517 nm and collected at 225° and 340°, excitation: 473 nm, at 90°.

where I_0 is the incident intensity of monochromatic light, n_{med} is the refractive index surrounding the particle, m is the refractive index of the bulk particle material (both functions of the incident wavelength) and r is the distance between the particles.

Taking into account the cosine law governing the light scattering from the glass and the SiFs themselves, we note that several factors play an important role in the angular-dependent scattering of light by SiFs-deposited surfaces observed here: (1) multiple scattering events: scattered light from a nanoparticle is reflected by another silver nanoparticle before scattering into the surrounding medium, (2) refractive index of the supporting substrate, and (3) excitation angle.

Moreover, it is well known that for fluorophores near interfaces with different refractive indices, a significant part of the fluorescence can be coupled into the medium of higher refractive index [29], with a unique angular dependence peaking at the critical angle [30]. Given that MEF is related to the surface plasmons' ability to scatter the coupled emission, the fluorescence emission through the high refractive index medium was further increased (enhanced emission) but also in an angular-dependent fashion, when

metallic nanoparticles are placed between the fluorophores and the glass interface.

As described in Section 1, the orientation of the dipole determines the extent of fluorescence enhancements observed from metallic surfaces. It is important to note that in our system here, fluorophore-labeled protein (4 nm in height) is randomly adsorbed onto SiFs and onto the glass substrate. In this regard, we expect an *ensemble-averaged* distribution of fluorophore orientations in our system due to the curvature of the silver islands. Thus, we expect that the observed enhancement emission is a result of those fluorophores which are positioned (depends on the direction of illumination) such that effective coupling of dipoles with the silver nanoparticles occur. Subsequently, due to the angular-dependent scattering nature of silver nanoparticles and the glass surface, the coupled emission is radiated in an angular-dependent fashion.

Since the angular-dependent enhanced fluorescence emission shown in Fig. 3 varies with the angle of observation, we next studied the photostability of FITC-HSA on SiFs at different observation angles from the back of the glass substrate, 225° and 340°, Fig. 4B. We again observe a higher photon flux (i.e., emission intensity is higher) from

FITC-HSA on SiFs at 225° than 340°, as also shown in Fig. 3 and the photograph inserts. However, we note that the photostability of FITC was indistinguishable at some observation angles (225° and 340° are shown).

Finally, we note the results of this study offer scientists with the opportunity for intensity-based angular-ratiometric surface assays, where the second emission intensity measured at an angle of choice could be used as a reference signal. The use of a second emission intensity also makes the measured fluorescence emission ratio independent of fluctuations in the excitation light and fluorophore loading; also offering scientists in different laboratories the opportunity to repeat the same experiment and obtain similar results.

3.1. Significance of these results for the interpretation of metal-enhanced fluorescence

It is important to comment on the angular-dependence of MEF in relation to the current interpretation of MEF. Several workers have described MEF as due to a fluorophore's modified radiative decay rate when in close proximity to metallic nanoparticles [8–10]. However, more recently Geddes and coworkers have described the mechanism of MEF as one where it is the particles (plasmons) themselves, which actually radiate the coupled-fluorophore quanta. From Fig. 3A, we can see that the coupled fluorescence intensity distribution is biased in the forward direction from SiFs, but it is not in the case of FITC immobilized solely on glass. This observation strongly suggests that the nanoparticles couple fluorescence and then radiate the fluorescence (elastically), the spatial intensity distribution dependent on the optical and scattering properties of the nanoparticles themselves. Subsequently, this observation further supports the mechanistic interpretations of MEF proposed by Geddes and coworkers [16].

To summarize the physical events for the angular-dependent MEF phenomenon: (1) excitation of fluorophores from air, (2) non-radiative energy transfer to the silver nanoparticles due to the coupling of the excited state with surface plasmons of the silver (induced mirror dipole), (3) emission from the fluorophore-plasmonic nanoparticle system into free-space and into the glass substrate, (4) coupling (and reflection) of fluorescence emission to/from the glass, Fig. 5.

4. Conclusions

We report the observation of angular-dependent MEF from fluorophores placed in close proximity to SiFs, a commonly used substrate. These observations were supported by our angular-dependent scattering studies, where we have shown that SiFs scatter light in an angular-dependent fashion which is slightly biased with respect to the direction of the excitation light. We note that the angular-dependent MEF does not follow the scattering properties/profile of the nanoparticles exactly, due to the heterogeneity of the sample. We have used two common excitation angles for surfaces, 45° and 90°. We observed angular-dependent metal-enhanced enhanced fluorescence with an up to 10-fold enhancement from FITC-HSA adsorbed onto SiFs when excited at these angles. We also observed similar photostability at the observation angles studied here.

Abbreviations

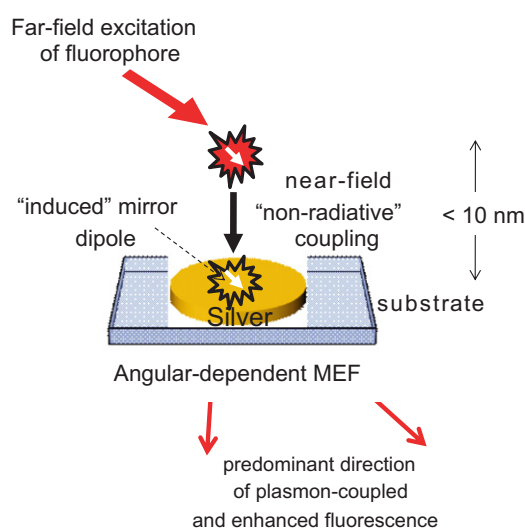|	
FITC-HSA	fluorescein isothiocyanate-labeled human serum albumin
MEF	metal enhanced fluorescence
RPM	radiating plasmon model
SiFs	silver island films
UPFT	unified plasmon-fluorophore theory

Acknowledgements

Fig. 5. Interpretation of angular-dependent metal-enhanced fluorescence. The intensity distribution is dependent on the angle of excitation, distance of fluorophore and dipole orientation from the silver nanoparticles, size and shape of the nanoparticles, refractive index of the substrate and the excitation wavelength.

References

[1] K.H. Drexhage, Berich. Bunsen Gesell. 72 (1968) 329.
[2] K.H. Drexhage, J. Luminesc. 1/2 (1970) 693.
[3] K.H. Drexhage, in: E. Wolfe (Ed.), Progress in Optics, North-Holland, Amsterdam, 1974, p. 165.
[4] W.H. Weber, C.F. Eagen, Opt. Lett. 4 (1979) 236.
[5] W.L. Barnes, J. Modern Opt. 45 (1998) 661.

[6] R.M. Amos, W.L. Barnes, Phys. Rev. B 55 (1997) 7249.

[7] J. Gersten, A. Nitzan, J. Chem. Phys. 75 (1981) 1139.

[8] P.C. Das, A. Puri, Phys. Rev. B 65 (2002).

[9] E. Dulkeith, M. Ringler, T.A. Klar, J. Feldmann, A.M. Javier, W.J. Parak, Nano Lett. 5 (2005) 585.

[10] R. Carminati, J.J. Greffet, C. Henkel, J.M. Vigoureux, Opt. Commun. 261 (2006) 368.

[11] Y.X. Zhang, K. Aslan, M.J.R. Previte, C.D. Geddes, Chem. Phys. Lett. 432 (2006) 528.

[12] M.H. Chowdhury, S.K. Gray, J. Pond, C.D. Geddes, K. Aslan, J.R. Lakowicz, J. Opt. Soc. Am. B-Opt. Phys. 24 (2007) 2259.

[13] T. Hatling, P. Reichenbach, L.M. Eng, Opt. Exp. 15 (2007) 12806.

[14] K. Aslan, V.H. Perez-Luna, Plasmonics 1 (2006) 111.

[15] T. Hayakawa, S.T. Selvan, M. Nogami, Appl. Phys. Lett. 74 (1999) 1513.

[16] K. Aslan, Z. Leonenko, J.R. Lakowicz, C.D. Geddes, J. Fluoresc. 15 (2005) 643.

[17] Y. Zhang, K. Aslan, M.J. Previte, C.D. Geddes, Chem. Phys. Lett. 432 (2006) 528.

[18] Y. Zhang, K. Aslan, M.J. Previte, C.D. Geddes, Appl. Phys. Lett. 90 (2007) 053107.

[19] K. Aslan, I. Gryczynski, J. Malicka, E. Matveeva, J.R. Lakowicz, C.D. Geddes, Curr. Opin. Biotechnol. 16 (2005) 55.

[20] Y. Zhang, K. Aslan, M.J.R. Previte, C.D. Geddes, AIP (2007) 173116.

[21] K. Ray, M.H. Chowdhury, J.R. Lakowicz, Anal. Chem. 79 (2007) 6480.

[22] M. Kawasaki, S. Mine, J. Phys. Chem. B 109 (2005) 17254.

[23] K. Aslan, S.N. Malyn, C.D. Geddes, J. Fluoresc. 17 (2007) 7.

[24] K. Aslan, P. Holley, L. Davies, J.R. Lakowicz, C.D. Geddes, J. Am. Chem. Soc. 127 (2005) 12115.

[25] K. Aslan, C.D. Geddes, Anal. Chem. 77 (2005) 8057.

[26] J. Yguerabide, E.E. Yguerabide, Anal. Biochem. 262 (1998) 137.

[27] M. Kawasaki, S. Mine, Chem. Lett. 34 (2005) 1038.

[28] M. Kerker, The Scattering of Light and Other Electromagnetic Radiation, Academic Press, New York, 1969.

[29] J. Enderlein, T. Ruckstuhl, S. Seeger, Appl. Opt. 38 (1999) 724.

[30] J.I. Gersten, A. Nitzan, Chem. Phys. Lett. 104 (1984) 31.